FACTA UNIVERSITATIS
Series: **Electronics and Energetics** Vol. 39, Nº 1, March 2026, pp. 123 - 136
https://doi.org/10.2298/FUEE2601123A

Original scientific paper

EVALUATION OF THERMAL EFFICIENCY OF A PVC-B SQUARE HONEYCOMB SOLAR COLLECTOR FOR RESIDENTIAL APPLICATIONS

Elson Avallone[1,2], Paulo Cesar Mioralli[2], Paulo Henrique Palota[2], Pablo Sampaio Gomes Natividade[2], Sílvio Aparecido Verdério Junior[3]

[1]Federal Institute of Science and Technology of São Paulo, Bauru-SP, Brazil
[2]Federal Institute of Science and Technology of São Paulo, Catanduva-SP, Brazil
[3]Federal Institute of Science and Technology of São Paulo, Araraquara-SP, Brazil

ORCID iDs:		
	Elson Avallone	https://orcid.org/0000-0001-9650-9239
	Paulo César Mioralli	https://orcid.org/0000-0001-8611-4356
	Paulo Henrique Palota	https://orcid.org/0000-0003-4459-7438
	Pablo Sampaio Gomes Natividade	https://orcid.org/0000-0001-6328-7457
	Sílvio Aparecido Verdério Junior	https://orcid.org/0000-0001-9695-7197

Abstract. *One square meter of solar surface produces approximately 63x10⁶ W/m² of energy and even with all the natural atmospheric filters, this energy is still very little explored, especially in thermal systems. Countries with an abundance of solar radiation still do not properly exploit this natural resource and when we look at poorer countries, this situation is even more worrying. The use of solar collectors for water heating represents significant economic and technological development throughout the world. In this work the PVC-B (Polyvinyl Chloride-Blue) lining honeycomb plate was converted into a solar collector, and its thermal efficiency was then analyzed. The cold-water inlet, hot water outlet and ambient temperatures, as well as the water flow and direct and reflected solar radiation from the ground are measured and these records are used to determine the energy absorbed by the water and incident on the solar collector. The average and maximum thermal efficiency of the PVC-B collector was 38.35% and 68%, respectively, with a maximum temperature of 42.94 °C. The collector in this study can be used both as a stand-alone system and as a hybrid system to support electric showers. The behavior of the solar collector studied here is analogous to a swimming pool collector, but with a cost of 73.18% lower. Even with a not so attractive average efficiency (38.35%), the low cost and simple construction make this equipment a great attraction for residential installation, as it can be built by the user*

Received March 26, 2025; revised May 28, 2025 and July 01, 2025; accepted July 15, 2025
Corresponding author: Elson Avallone
Federal Institute of Science and Technology of São Paulo, Bauru-SP, Brazil and Federal Institute of Science and Technology of São Paulo, Campus Catanduva-SP, Brazil, and Campus Bauru-SP, Rua Severino Lins, 7-10 - Vila Aviação – Bauru-SP - Brazil
E-mail: elson.avallone@ifsp.edu.br
*An earlier version of this paper was presented at the 9th Virtual International Conference on Science, Technology and Management in Energy (eNergetics-2023), November 23-24, 2023, in Nis, Serbia [1].

himself and used to heat water for low-income families, which is a promising result for a low-investment equipment, compared to commercial solar collectors (FPC).

Key words: *Solar collector, prototype, PVC-B, honeycomb, thermal efficiency*

NOMENCLATURE

Symbol	*Description*	*Unit*
A	Front and rear collector area	[m²]
cp	Specific heat of water at constant pressure	[J/kg.K]
G_{dir}	Direct solar heat flow	[W/m²]
G_{refl}	Solar reflected heat flow	[W/m²]
m	Mass flow	[kg/s]
T_h	Hot water temperature	[°C]
T_c	Cold water temperature	[°C]
T_∞	Ambient temperature	[°C]
$\dot{Q}_a$	Absorbed heat rate by the collector	[W]
$\dot{Q}_i$	Incident heat rate by the collector	[W]
$\dot{Q}_u$	Incident heat rate on the upper surface of the collector	[W]
$\dot{Q}_l$	Incident heat rate on the lower surface of the collector	[W]
$F_{R(\tau\alpha)}$	Heat removal factor	[dimensionless]
α	Solar collector inclination	[°]
η	Thermal efficiency of the solar collector	[dimensionless]

1. INTRODUCTION

Brazil leads the renewable energy market in Latin America in solar water heating and has great potential for growth in this technology due to its simplicity and high economic viability. Despite the leadership in the thermal production sector for water heating and the abundance of sunlight in Brazil, many families still use electrical equipment to heat water for bathing, thus increasing energy consumption, generating an increase in electricity bills and drastically overloading the industrial electrical system, especially during peak consumption times. When we analyze this scenario for low-income families, the situation is even more critical, as they have neither knowledge of alternatives for reducing electricity costs nor financial resources to purchase industrialized equipment, since 22.8% of the household budget is consumed only with said electricity [2]. Brazilian Law MPV 1162/2023 deals with the installation of photovoltaic panels, however, the aforementioned Law does not cover thermal systems, thus losing the capacity for exploration in the sector and reducing the financial situation of the population due to the lack of incentives in thermal systems. Among the renewable energy sources used until the end of 2015, investments were distributed between 2.3% in nuclear energy and 19.3% in all other renewable energies, demonstrating great solar, wind and geothermal energy potential [3]. At the end of 2009, thermal energy storage capacity was approximately 600 MW and at the end of 2013 a total of 3.6 GW [4]. In 2016, production capacity increased to 456 GW, distributed across 652 million m² of installed collectors [5]. In the study of [6], the main use of solar energy is restricted

to domestic water heating using solar collectors, as it has a low environmental impact and a significant reduction in the use of conventional energy sources. Reducing family electricity demand leads to social improvement, environmental preservation, the possibility of creating jobs and financial savings, in addition to a significant reduction in greenhouse gas emissions. A case study revealed that the cost-benefit of using photovoltaic energy technology for heating water in a single-family home through a survey of the number of people living in the building, as well as the respective per capita water consumption, resulted in the use of this type of energy being economically viable, as the results demonstrated a significant reduction in the cost of energy consumed in the home [7] The International Conference Rio +20 [8] reports on the construction of sustainable cities, including the rational use of energy, with effective control by public authorities. The residential sector has an average consumption of 24% of the total electricity consumed [5]. The use of a hybrid system consisting of solar collectors linked to electric showers allows a 10% reduction in electricity costs [9]. General Electric published a report stating that the use of renewable energy can quickly change the trajectory of climate change. The generation and distribution of renewable energy must provide an economically viable, renewable and reliable energy matrix and the most effective way is diversification [10]. As Brazil's energy matrix is mostly hydroelectric, the use of solar energy for residential water heating corresponds to savings of 70% in electricity consumption [11] and the application of new technologies makes it possible to reduce fossil fuels for generation and electrical energy distribution [12]. The Flat Plate Collector (FPC) is used in moderate heating situations, taking advantage of solar radiation, with little maintenance, widely applied in water heating in buildings and various industrial processes. [13] conducted tensile testing versus deformation, analyses by infrared spectrometry, and degradation kinetics by thermogravimetry on samples taken from the naturally aged plates of a polyvinyl chloride-based compound used in the absorber plates of low-cost solar collectors after 5 years of use and found that they functioned normally, without leaks and heating water up to 50°C. The authors [14] studied the effect of thermal conductivity and collector area for PVC-B (PVC-B: Polyvinyl Chloride-Blue), PB (PB: Polybutene), PP-R (PP-R: Polypropylene Random Copolymer) and PVC-CB: (Polyvinyl Chloride-Carbon Black) and found that the differing thermal conductivity materials have indicated that there is no difference of the materials on collector thermal efficiency, but only due areas of the panel.

The goal of this study is to build a PVC-B square honeycomb solar collector and measure its thermal efficiency.

The work describes in section 2 the methods and procedures used in the research, including data collection and analysis. Section 3 presents the data obtained in the research, accompanied by figures. It interprets the results, relating them to the existing literature and highlighting the contributions of the study. Section 4 summarizes the main findings and their implications.

2. METHODOLOGY

The solar collector studied was built with a PVC-B (Polyvinyl Chloride-Blue) square honeycomb plate, whose internal channels provide water circulation, with better heat distribution (Fig. 1(a)). PVC-B tubes with slots are fixed to the ends of the linen with high-resistance PVC-B glue and epoxy resin, as shown in Fig. 1(b).

Fig. 1(a) PVC-B square honeycomb

Fig. 2(b) Installation of PVC-B pipes with slots at the ends of the plates [11]

The solar collector was coated with high absorptivity matte black paint, used to manufacture commercial solar collectors. The complete assembly is shown in Fig. 3.

Fig. 3 Complete assembly

The angle α in Fig. 4 is determined according to Technical Standard ABNT-NBR 15569 [15], [16] and [17] with an inclination of the local latitude of 21°8′16″ south plus 10°. The addition of 10° of inclination in the local latitude compensates for the annual translational movement of the earth in the transition from winter to summer and vice versa. Water is pumped between the PVC-B collector and the reservoir, (Fig. 4), maintaining a constant flow.

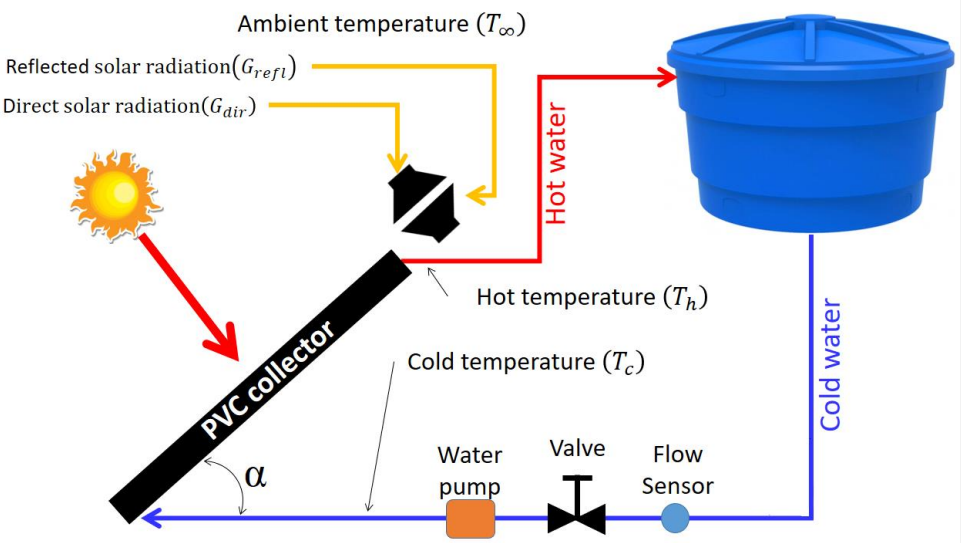

Fig. 4 Schematic diagram of the test bench

The electric pump flow adjustment is carried out through the manual valve and monitored by the Arduino serial monitor [18].

The temperatures of hot water (T_h) and cold water (T_c) are measured with DS18B20 encapsulated sensors [19] and installed in the PVC-B connections at the hot water outlet and cold water inlet, respectively. The ambient temperature is measured with the same sensor (DS18B20) installed in a tube open at both ends, thermally isolated and with forced ventilation. The calibration of these sensors is defined by the suppliers.

The radiation incident from the sun and reflected from the ground are measured using thermal radiometers constructed according to [20], [21], [22], [23] and [24], installed with the same inclination as the angle α. Although these radiometers are of simple construction, they have excellent agreement with industrialized equipment, a fact proven by publications [20], [21], [22], [23] and [24]. The calibration and validation process was also presented by [21] pp.19 and are the same as those developed by [20], [21], [22], [23] and [24]. In summary, the calibrations of the radiometers were conducted at IPMet [25] in the city of Bauru, where the sensor to be calibrated was installed next to the reference sensor. The data collected by the sensors were plotted, generating a point cloud in which the "x" axis represents the sensor to be calibrated and the "y" axis the reference sensor. Using the point cloud, a trend line was drawn that generated a calibration equation. The sensor to be calibrated works by the thermal principle that measures the temperature difference over a blackened aluminum disk and the ambient temperature. The temperature difference between the blackened disk and the ambient temperature is inserted into the calibration equation, thus converting it into solar radiation in W/m2.

To measure the volumetric flow, a YF-S401 sensor [26] was used, calibrated on a test bench, and the results were converted into mass flow. This calibration can be seen at PhD thesis of author [27]. The circuit flow was set at 0.017 kg/s by the valve in Fig. 4 and visualized by the Arduino serial monitor.

The electronic circuit diagram developed for this work is shown in Fig. 5. A similar assembly was developed by [28].

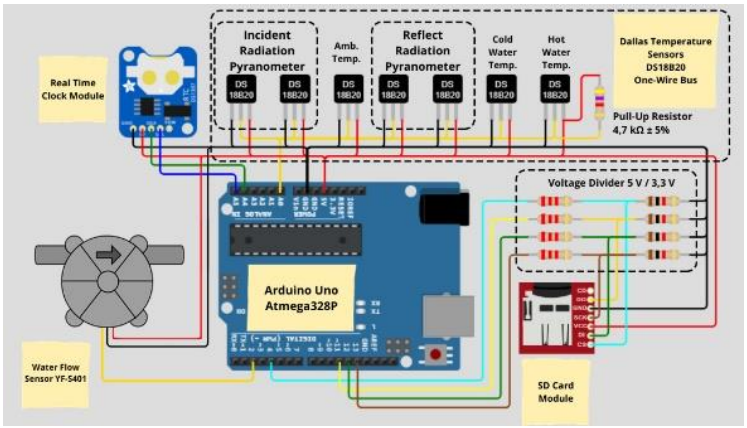

Fig. 5 Schematic diagram of the Dataloger/Arduino

The shield with the Arduino, RTC module, SD module and terminals is shown in Fig. 6.

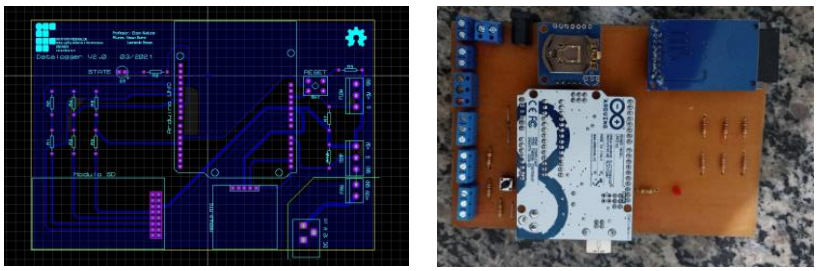

Fig. 6 Shield with Arduino, RTC module, SD module and terminals

2.1. Mathematical formulation

To evaluate the heat flow absorbed by the solar collector, the summarized First Law of Thermodynamics was used [15], [29], [30], presented in Equation 1.

$$\dot{Q}_a = \dot{m}.cp.(T_h - T_c) \tag{1}$$

The $\dot{Q}_a$ in the Equation (1) is the heat flow absorbed by water [W], $\dot{m}$ the mass flow rate of water [kg/s] using specific mass of water ρ = 1000 kg/m^3, cp the specific heat of water at constant pressure with a value fixed at 4186 J/kg.K, T_h the temperature at the hot water outlet [ºC] and T_c the temperature at the cold water inlet [ºC]. Temperatures, as well as all other physical properties, are measured through the data acquisition system shown in Fig. 5. We consider the variation in the specific heat of water to be negligible, since its variation with the largest temperature difference of approximately 7.63 °C at 14:05 hours, during the test, generated a very small variation in heat capacity in the order of 0.024%, equivalent to 1.0 J/Kg.K.

The total solar flux incident on the collector $\dot{Q}_i$ is determined by adding the heat flux on the upper surface $\dot{Q}_u = G_{dir} \times A$ and the heat flux on the lower surface $\dot{Q}_l = G_{refl} \times A$ presented in Equation 2.

$$\dot{Q}_i = \dot{Q}_u + \dot{Q}_l \tag{2}$$

where the direct (G_{dir}) and reflected (G_{ref}) radiation are measured using the radiometer developed by [28], where the calibration is presented, and A is the upper and lower area (A = 0.7381 m^2) of the collector with dimensions 0.613 x 1.204 m. The PVC-B solar collector does not have the glass cover and protective box, found in commercial collectors, solar intensity is measured both by direct incidence and reflected by the ground, that is, the total available heat flux is determined by the already defined Equation 2. Direct and reflected solar radiation are also measured through the data acquisition system shown in Fig. 5.

To determine the thermal efficiency of the PVC-B collector, Equation 3 is used.

$$\eta = \frac{\dot{Q}_a}{\dot{Q}_i} \times 100 \tag{3}$$

Which η is the thermal efficiency of the collector in percentage.

The heat removal factor of the solar collector measures the amount of heat removed by the collector to the water. The books by Dr. Soteris Kalorigou [15] (pp. 173) and Duffie & Beckman [29] (pp. 263) present the equations to determine this factor. This equation was also extensively used in the Ph.D. thesis of [27].

Equation 4 presents the graphical relationship to determine the heat removal factor of the solar collector, with the thermal efficiency (η) being a function of the variation in cold and ambient temperatures and the radiation incident on the collector on both the upper and lower surfaces, as shown in Equation 4.

$$\eta = f\left(\frac{T_c - T_\infty}{(G_{dir} + G_{ref})}\right) \tag{4}$$

The removal factor called $F_{R(\tau\alpha)}$ is the intersection point of the average line of the experimental points with the "y" axis and represents the initial efficiency of the solar collector, presented by [15] (pp.223).

3. Results and Discussion

Fig. 7 shows the temperature profiles of cold-water inlet, hot water outlet and ambient temperature. The cold, hot and ambient temperatures measured in forced circulation are, respectively, the cold-water inlet, lower region of the collector, hot water outlet, upper region and ambient temperature. Fig. 7 shows the transient variations of the cold inlet and hot outlet temperatures. The ambient temperature influences the collector efficiency, since equation 4 presents the efficiency as a function of the variation of the cold water and ambient temperatures divided by the incident solar radiation. The oscillations in Fig. 7 and Fig. 9 refer to the passage of clouds in the experiment region.

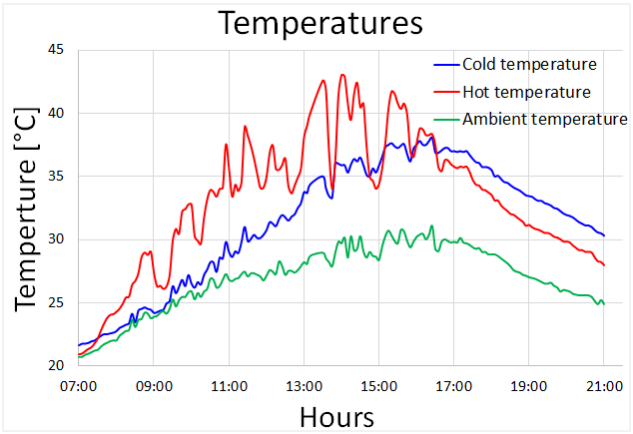

Fig. 7 Solar collector temperature profiles

The two radiometers, installed with inclination angle α, shown in Fig. 8 measure direct solar radiation and that reflected from the ground, respectively.

Fig. 8 Radiometers for incident and reflected radiation

The incident and reflected transient radiations are shown in Fig. 9, where the oscillations indicate clouds.

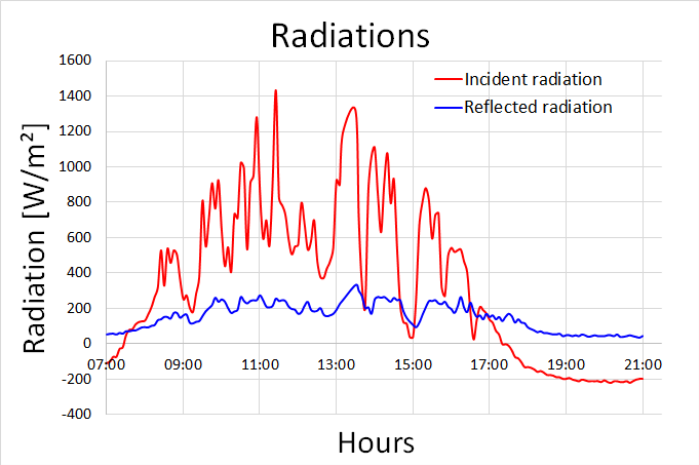

Fig. 9 Solar radiation measured with the two radiometers

The incident and absorbed energy are shown on Fig. 10. The interesting about this graph is the interval between energies, representing the losses in the solar collector, with an average of 298.33 W, relatively small losses for such a simple and inexpensive system.

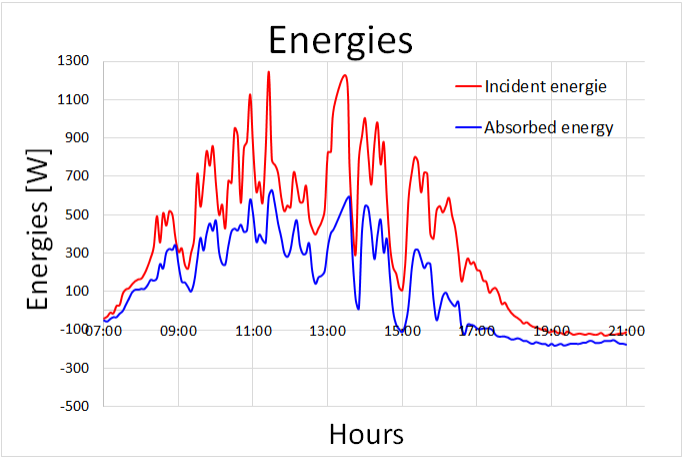

Fig. 10 Energy incident and absorbed by the solar collector

The difference between the incident energy and the absorbed energy represents the losses in the collector, which can be better seen on Fig. 11, highlighted in yellow.

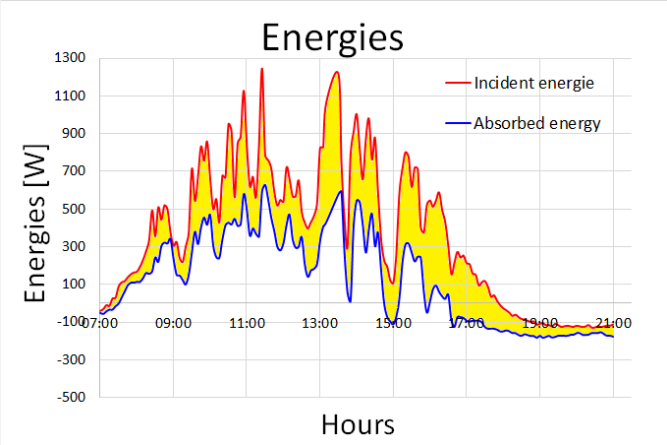

Fig. 11 Energy losses in the solar collector

For a solar energy analysis, the sums of accumulated incident and absorbed energy in the collector are presented in the graph on Fig. 12, with maximum values of 17.58 MJ and 6.64 MJ, respectively. The yellow region also represents the energy losses of the solar collector studied.

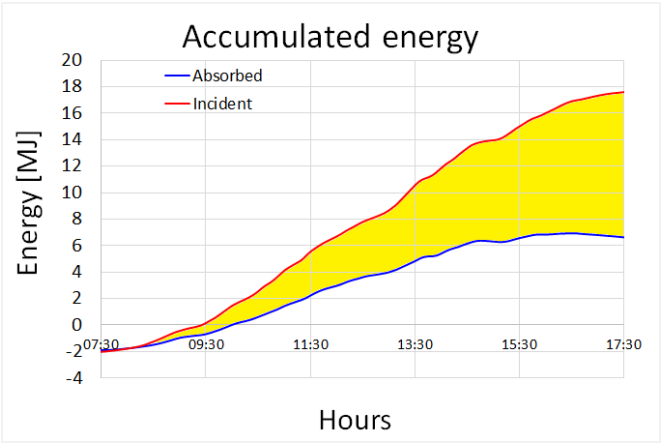

Fig. 12 Accumulated energy incident and absorbed in the solar collector

The transient efficiency of the solar collector is shown in Fig. 13. The sudden drop at 15:00 refers to the passage of many clouds over the experiment site, also visualized in the radiation graph in Fig. 9.

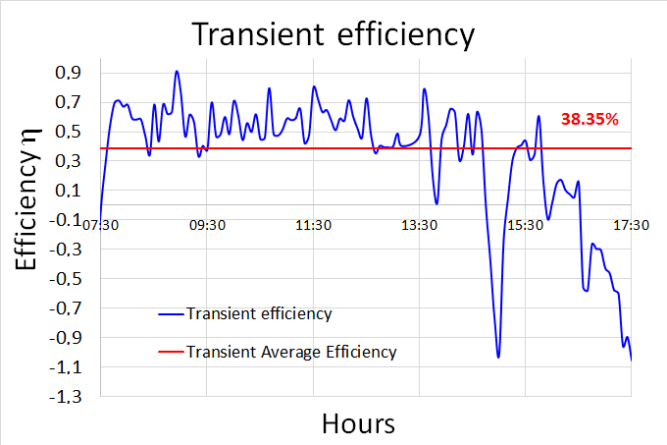

Fig. 13 Transient efficiency of the PVC-B solar collector

Fig. 13 also shows the average value of 38.35% in PVC-B collector efficiency.

In this paragraph the authors highlight the influence of clouds on the experiment. When clouds pass over the collector, there is a reduction in the temperatures shown on Fig. 7, which leads to a variation in the incident and energies absorbed by the collector, as shown on Fig. 10. In Fig. 13, a transient variation in the collector efficiency can be observed. Fig. 11 shows the incident, absorbed and lost transient energies. Another way to analyze this is through Fig. 12, which shows the accumulated, incident, absorbed and lost energy in the solar collector studied.

Fig. 14 presents a comparative graph between the studied collector, where the black points represent the experimental points, the red line is the trend line of the said points, and the intersection with the vertical axis is the initial efficiency, with an approximate value of 0.68, that is, 68%. The green and blue lines represent the pool solar collector and the solar collector with glass cover, respectively, according to the data published by Kalogirou [15] (pp. 243). A comparative evaluation between the lines shows that the studied collector has a behavior analogous to the pool solar collector. The angular coefficient of the red medium line is equivalent to the losses of the equipment to the environment, which creates a significant slope compared to other types of solar collectors.

Taking as a reference a loss of -40.19 of the studied PVC-B collector (red line), when compared with commercial collector with a glass cover of -8.0822 described by Kalogirou [15] (pp. 243, blue line in Fig. 14), it is observed that there is a loss 79.9% greater for the studied collector. This indicates that the thermal reservoir and the glass cover provide a significant increase not only in efficiency but also in reducing heat losses to the environment. Similarly, comparing the losses of 40.19 from the studied collector with the losses of -20.581 from the swimming pool collector described by Kalogirou (green line in Fig. 14), it can be seen a loss of 48.12% greater than that of the swimming pool collector, as the pool collector is made from a material similar to PVC.

The graph of the studied solar collector, presented in Fig. 14, has a behavior analogous to a swimming pool collector, as both types of collectors presented touch the axes of the abscissas and ordinates.

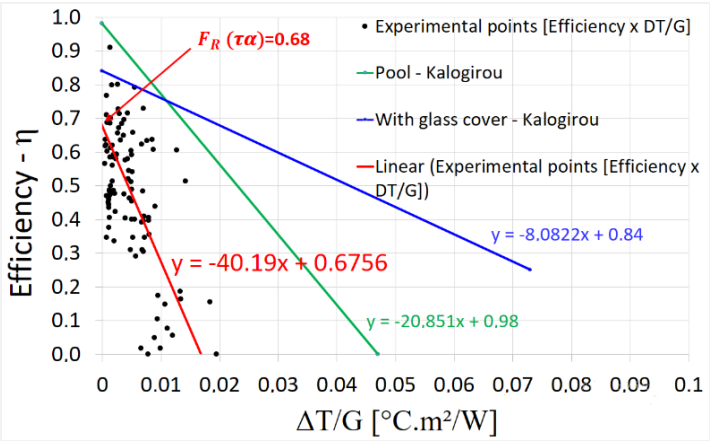

Fig. 14 Efficiency x $\Delta T/G$

The absence of these protective features reduces the collector's efficiency, but also drastically reduces the equipment's production costs. An installation as a proposal to reduce the costs of the studied system for the user can be seen in Fig. 15.

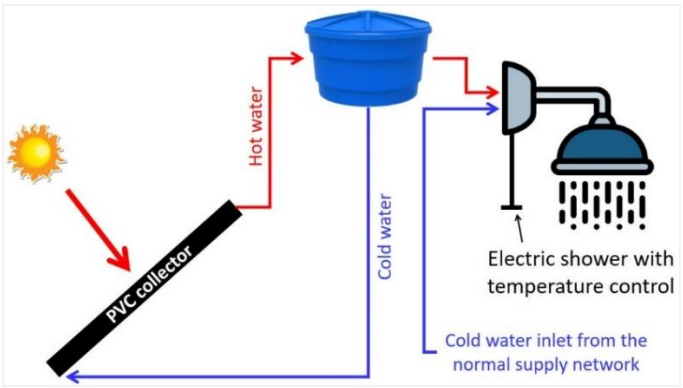

Fig. 15 The installation of solar heating system using a commercial electric shower

Cold water enters the solar collector through the lower region. The solar collector heats the water, generating an upward movement, raising it to the water tank, which functions as a thermal storage device. The hot water in the water tank remains in the upper region due to the difference in density and is collected in this same region for the electric shower, where the temperature of the shower must be regulated by an electric control, as used in commercial electric showers. The electric control is activated only on days with lower temperatures for a pleasant shower, which only on these days will there be electricity costs. In high summer temperatures, the hot water coming from the water tank can generate an uncomfortable shower, with excessive temperature, which requires a cold-water system to regulate the water temperature for a comfortable shower.

4. CONCLUSION

The build PVC-B solar collector has an average efficiency of 38.35% and initial efficiency of 68% with a maximum temperature of 42.94 °C. As the solar collector does not have a glass cover or a thermal reservoir, there is a large loss of heat to the environment, which justifies the large angular coefficient of -40.19 of the red curve in the graph in Figure 14, that is, there is no degradation of the material during the thermal process, but only heat loss to the environment. Commercial flat plate solar collector (FPC), which are built with copper or aluminum piping with fins for greater absorption of solar heat flow installed in a metal box with a glass cover, have an average efficiency of 60% [15] and [31]. The efficiency of the PVC-B collector has an interesting result, as it is a cheap project. The application of this solar heater collector makes it possible to use it for low-income families and even with a not-so-high efficiency, it can be used as a hybrid system, to support electric showers with a dimer to control the electric resistance as could be seen in Fig. 15, which could reduce electric power bill. Another important factor is that the solar collector is a do-it-if yourself with easy-to-find materials and simple assembly, eliminating the use of metal welding. The system proposed for this work uses a single water tank, for both hot and cold water, using stratified thermal separation. As a result, low-income families will not have to spend with another reservoir for storing hot water. The solar collector studied here has a behavior like a swimming pool solar collector. Comparing the built area and cost, the commercial collector has an area of 0.66 m^2 with a cost of US$ 151.52/m^2, while the collector studied has an area of 0.7381 m^2 with an estimated cost of US$ 40.64/m^2, i.e. represents 73.18% cheaper when compared to the commercial collector. It is important to consider that the collector studied requires maintenance, painting, every 3 years. Painting is an important factor in the durability of the solar collector studied, since in its absence, the PVC-B solar collector is exposed to ultraviolet rays, which would cause its degradation. This will generate the need to repaint it periodically. Another attraction for this equipment is the average losses of 287.66 W from 7:00 to 17:30. As it is a device without a glass cover and without a protective box, it can be considered that these are very small losses. The PVC-B solar collector works best in regions close to the equator due to greater solar incidence. Even with relatively higher temperatures than in the northern hemisphere, there are still low temperatures, such as below the Tropic of Capricorn, however, the solar collector studied will function adequately at any latitude. Furthermore, the poorest regions in the world are located close to the equator and these devices can reduce electricity bills. A government awareness plan for low-income families would be a good global practice to increase the use of solar collectors for water heating.

Acknowledgement: *To the Federal Institute of Education, Science and Technology of São Paulo, Campus Catanduva-SP and Campus Bauru-SP for the constant support and encouragement.*

REFERENCES

[1] K. O. M. Bueno, P. C. Mioralli, P. H. Palota, P. S. G. Natividade and S. A. Verdério Júnior, "Thermal Efficiency of a PVC Honeycomb Solar Collector", In Proceedings of the 9th Virtual International Conference on Science, Technology and Management in Energy, vol. 1, Complex System Research Centre, Niš, Serbia, 2023, p. 117-122.

[2] O. A. Teixeira, O. Vital Brazil and P. M. Araújo, "The Access of Low Icome Population to the Thermal Solar Energy by Energy Efficiency Projects", *ABENS - Associação Brasileira de Energia Solar* Fortaleza - Brazil, vol. 1, pp. 1-7, 2007.

[3] A. Zervos and C. Lins, "REN 21: Global Status Report 2017". REN 21 - Renewable Energy Policy Network for the 21st Century, 2017.
[4] M. Van der Hoeven, "IEA - International Energy Agency". IEA, 2014.
[5] Ê. B. Pereira *et al.*, "Atlas brasileiro de energia solar", INPE - Instituto Nacional de Pesquisas Espaciais, 2017.
[6] B. Metz, O. Davidson, P. Bosch, D. Rutu and L. Meyer, *Climate Change 2007: Mitigation. Contribution of Working Group III to the Fourth Assessment Report of the Intergovernmental Panel on Climate Change*, 1ª. Canada: Cambridge University Press, 2007.
[7] L. D. S. Maia, W. P. Miranda, and É. C. N. M. Pinheiro, "Sizing of a Water Heating System in a Single-Family Residence through Solar Energy Capture: Case Study", *IJAERS*, vol. 8, no. 6, p. 134-144, 2021.
[8] United Nations, "A Rio+20 e a Construção de Cidades Sustentáveis - A Rio+20 e a Construção de Cidades Sustentáveis", 2012.
[9] A. Oliveira, R. Jordão, R. Resende, R. Caputo and R. da Silva, "Projeto de Residência com melhor aproveitamento energético - Residential project with better energy use", *O Setor Elétrico*, no. 109, 2015.
[10] S. Winoker, "GE Announces Plans to Form Three Public Companies". General Eletric, 2021.
[11] ASBC, "Sociedade do Sol". ASBC, 2001. [Online]. Available at: http://www.cds.unb.br/obmts
[12] EPE, "Nota técnica DEA 13/15 - Demanda de Energia 2050". Empresa de Pesquisa Energética (EPE), 2016.
[13] B. R. Prado, T. T. Pinto, E. G. Fernandes and J. R. Bartoli, "Envelhecimento e caracterização de compostos de PVC usado em placas de coletores solares de baixo custo", *11° CBPol* - Campos do Jordão - SP - Brazil: Associação Brasileira de Polímeros, vol. 1., p. 5609-5614, 2011.
[14] W. Ariyawiriyanan *et al.*, "Thermal Efficiency of Solar Collector Made from Thermoplastics", *Energy Procedia*, vol. 34, p. 500-505, 2013.
[15] S. A. Kalogirou, *Solar Energy Engineering*, 1ª., vol. 1. United States of America: British Library Cataloguing-in-Publication, 2009.
[16] ABNT, *NBR 15569: Sistema de aquecimento solar de água em circuito direto - Projeto e instalação - Direct circuit solar water heating system - Design and installation*. 2008, p. 18.
[17] NBR 15569, "Sistema de aquecimento solar de água em circuito direto — Requisitos de projeto e instalação". Associação Brasileira de Normas Técnicas, 2021.
[18] Arduino, "Arduino UNO", Arduino, 2015.
[19] Maxim, "DS18B20 Dallas Semiconductor", Dallas Semiconductor, 2012.
[20] E. Avallone, P. C. Mioralli, V. L. Scalon, A. Padilha and S. del R. Oliveira, "Thermal Pyranometer Using the Open Hardware Arduino Platform", *Int. J. Thermodyn.*, vol. 21, no. 1, p. 1-5, Mar. 2018.
[21] E. Avallone *et al.*, "Radiômetro solar de baixo custo usando a plataforma aberta Arduino", *Coleção desafios das engenharias: Engenharia mecânica*, 1º ed, Atena Editora, p. 79–91, 2021.
[22] R. P. Garcia, E. Avallone, C. Pansanato, G. B. Gonçalves, M. C. Ito, V. L. Scalon, "Thermal Radiometer using LM35 Analog Sensors, Connecting to an Arduino Board", In Proceedings of ENCIT, Águas de Lindóia - SP: ABCM, 2018, p. 1-8.
[23] C. Pansanato, G. B. Gonçalves, M. C. Ito, V. L. Scalon, E. Avallone and R. P. Garcia, "Low Cost Thermal Pyranometer using Dallas DS18B20 Sensor and Arduino", In Proceedings of ENCIT, Águas de Lindóia - SP: ABCM, 2018.
[24] V. L. Scalon, E. Avallone, C. Pansanato and M. Ito, "Development of a Low Cost Pyranometer for Solar Radiation Measurements", ABCM, 2017.
[25] IPMet Unesp, "IPMet Unesp". 2019.
[26] DFRobot Electronic Product, "Flow sensor - YF-S401-1/8".
[27] E. Avallone, "Estudo de um coletor solar, tipo tubo evacuado modificado, utilizando um concentrador cilíndrico parabólico (CPC)", PhD Thesis, Universidade Estadual Paulista "Júlio de Mesquita Filho" - UNESP/FEB, Brazil, 2017.
[28] E. Avallone, P. C. Mioralli, V. L. Scalon and A. Padilha, "Thermal Pyranometer using the Arduino Platform for Data Acquisition", In Proceedings of the 4th International Conference on Contemporary Problems of Thermal Engineering, Katowice, Poland, 2016, p. 303-311.
[29] J. A. Duffie e W. A. Beckman, *Solar Engineering of Thermal Process*, 4ª., vol. 1. USA: John Wiley & Sons, 2013.
[30] F. Struckmann, "Analysis of a Flat-plate Solar Collector", in *Heat and Mass Transport*, Lund, Sweden, 2008.
[31] L. de O. Tavares, V. V. Dimbarre, F. M. Biglia, F. B. C. Cruz, P. H. D. dos Santos and T. A. Alves, "Análise experimental do desempenho térmico de um coletor solar do tipo placa Plana", em *IA nas engenharias*, em 1, vol. 1. Paraná - Brazil: APREPRO - Associação paranaense de engenharia de produção, dez. 2023, p. 1-11.